

Few-Shot Classification By Few-Iteration Meta-Learning

Ardhendu Shekhar Tripathi
 Computer Vision Lab
 ETH Zurich, Switzerland

ardhendu-shekhar.tripathi@vision.ee.ethz.ch

Luc Van Gool
 Computer Vision Lab
 ETH Zurich, Switzerland

vangool@vision.ee.ethz.ch

Martin Danelljan
 Computer Vision Lab
 ETH Zurich, Switzerland

martin.danelljan@vision.ee.ethz.ch

Radu Timofte
 Computer Vision Lab
 ETH Zurich, Switzerland

radu.timofte@vision.ee.ethz.ch

Abstract

Learning in a low-data regime from only a few labeled examples is an important, but challenging problem. Recent advancements within meta-learning have demonstrated encouraging performance, in particular, for the task of few-shot classification. We propose a novel optimization-based meta-learning approach for few-shot classification. It consists of an embedding network, providing a general representation of the image, and a base learner module. The latter learns a linear classifier during the inference through an unrolled optimization procedure. We design an inner learning objective composed of (i) a robust classification loss on the support set and (ii) an entropy loss, allowing transductive learning from unlabeled query samples. By employing an efficient initialization module and a Steepest Descent based optimization algorithm, our base learner predicts a powerful classifier within only a few iterations. Further, our strategy enables important aspects of the base learner objective to be learned during meta-training. To the best of our knowledge, this work is the first to integrate both induction and transduction into the base learner in an optimization-based meta-learning framework. We perform a comprehensive experimental analysis, demonstrating the effectiveness of our approach on four few-shot classification datasets.

1. Introduction

Unlike humans, most machine learning techniques require thousands of examples to even achieve acceptable performance on the same task. The problem of few-shot learning, *i.e.* learning tasks from scarce data, has therefore gained significant interest in recent years [30, 27, 6]. Among current directions, few-shot classification [4] aims at learning a classifier given only a few labeled examples. In the extreme,

there might only be a single example of each class. One promising direction in few-shot learning is to design methods that gain experience from learning to solve other similar tasks in order to better learn the task at hand. This is generally referred to as meta-learning [13], aiming to ‘learning to learn’ how to solve individual tasks.

Meta-learning itself covers a wide diversity of methods. In few-shot classification, two types of approaches have been particularly successful, namely metric learning [30, 27, 28] and optimization-based [6, 23, 22, 15, 1]. While the former learn an embedding space, the latter aim at optimizing a set of model parameters to solve the specific task. We build on the optimization-based paradigm, as it allows for the integration of powerful task-specific learning formulations that require objective minimization. We consider the setting with two main modules, (i) a meta-network and (ii) a base learner. The meta-network generally learns a feature representation across a distribution of tasks. The base learner, on the other hand, performs the task-specific adaptation. To ensure practical meta-learning, the adaptation process must be both, efficient and differentiable. Recent works have explored closed form solutions [1] and implicit differentiation of the optimality conditions [15]. However, these methods lack significant flexibility in terms of the choice of base learner objective. In this work, we therefore explore an alternative approach.

We propose a base learner employing unrolled optimization. To this end, we utilize the steepest descent algorithm, combined with quadratic approximation and effective initialization, which ensures reliable convergence within only a few iterations. Our optimization strategy allows for greater flexibility in the choice of the base learner objective. Specifically, we formulate a parametrized objective that is *learned* during meta-training. Moreover, as made possible by our meta-learning framework, we investigate the integration of trans-

ductive learning strategies into the base learner itself. Unlike previous optimization-based methods, which only employ support images, our base learner incorporate information from the query samples, both, during meta-training and inference. Our meta-learning approach is efficient, achieving $200\times$ faster inference time compared to state-of-the-art fine-tuning based methods [5].

Contributions: Our work contains the following main contributions. (i) We propose FIML, a flexible meta-learning framework based on an efficient unrolled optimization strategy. (ii) We introduce a learnable inductive objective, employed by the base learner. (iii) We integrate transductive learning into the base learner. (iv) We develop a method for leveraging spatial dense features for few-shot classification. To validate each of our design choices, we perform extensive ablative experiments. Further, we evaluate our approach on four few-shot classification benchmarks, setting a new state-of-the-art in several settings.

2. Related Work

Current state-of-the-art meta-learning methods can be broadly categorized into two main categories - metric-based and optimization-based. The metric-based methods [30, 27, 28, 11] aim at learning a common embedding space where it is easy to distinguish between different categories through a distance metric. Noticibly, the few-shot classification problem can also be modelled as a graph matching problem. Garcia *et al.* [7] and EGNN [10] explore graph neural representations for few-shot classification. Optimization-based meta-learning methods aim to learn to adapt a model to a given task. Notably, a family of MAML [6] based methods adapt a set of prior model parameters to the task through first-order optimization [18]. Recently, Zintgraf *et al.* [31] proposed an extension to MAML called CAVIA that is less prone to meta-overfitting. CAVIA partitions the model parameter into task-specific context parameters and the task-agnostic shared parameters and updates only the context parameters at test time. In a similar direction, Rajeswaran *et al.* [22] suggest an implicit MAML variant that mitigates the issue of differentiating through the task-specific inner-learner by drawing upon implicit differentiation.

Another line of research partitions the parameter space into task-agnostic and task-specific parameters. The latter are learned explicitly for each task, while the former remain fixed. Bertinetto *et al.* [1] utilize a closed-form solution of the base learner, formulated as a ridge regression problem. More recently, MetaOptNet [15] employs a Support Vector Machine (SVM) as the task-specific model. Gradients are back-propagated through the SVM learning during meta-training using implicit differentiation of the optimality conditions of the convex problem. While achieving promising performance, both these works [15, 1] are restricted to specific types of task-specific models. In contrast, our approach

allows for more general and flexible learning objectives. This enables us to, for instance, integrate entropy-based transductive learning during the meta-training stage. Moreover, in contrast to previous optimization-based few-shot classification methods, we propose to learn aspects of the task-specific learning formulation itself.

3. Method

3.1. Formulation

Our meta-learning approach follows the paradigm in [15, 1] by having two components: the base learner and a meta-learner. The aim of the base learner is to learn to perform a new task. It is, therefore, task-specific. The meta-learner, on the other hand, generalizes over a vast number of tasks. The main goal of the meta-learner is to learn a representation that is used by the task-specific base learner. In a few-shot classification setting, a task $T = \{S, Q\}$ is characterized by a set of unlabeled *query* images $Q = \{\tilde{x}_j, \tilde{y}_j\}_{j=1}^{\tilde{N}}$ which need to be classified, given only a few labeled image exemplars, called the support set $S = \{x_j, y_j\}_{j=1}^N$. Here x_j and \tilde{x}_j are the j^{th} image samples in the support and query sets, respectively. The corresponding labels in the support and query sets are denoted by y_j and \tilde{y}_j , respectively. The support set contains $N = k \times n$ image-label pairs, *i.e.* n examples for each of the k classes. Such a setting is called a k -way, n -shot classification problem. The query set Q contains \tilde{N} image-label pairs with the images sampled from the same class set as the support samples. For a given task, the support and query labels share the same label space $L = \{1, 2, \dots, k\}$. The task support samples and the query samples for task T are sampled from a data split D of dataset \mathcal{D} . Here, $D \in \{D_{\text{train}}, D_{\text{val}}, D_{\text{test}}\}$ and, D_{train} , D_{val} and D_{test} are the train, validation and test splits of \mathcal{D} . The dataset \mathcal{D} also defines the domain of the few-shot classification problem. The train, validation and test data splits are mutually disjoint and contain no common samples. Further, to measure the meta network's generalization to unseen categories, the class sets for the train, validation and test splits (C_{train} , C_{val} and C_{test} respectively) are chosen to be pairwise disjoint.

The aim of the base learner \mathcal{B} is to learn the optimal task specific base network b_{θ^*} conditioned on the meta network m_{ϕ} . The general form of the base learner \mathcal{B} is given by,

$$\mathcal{B}(T; m_{\phi}) := \theta^* = \arg \min_{\theta} \mathcal{L}_{\text{base}}(T, b_{\theta}; m_{\phi}), \quad (1)$$

where $\mathcal{L}_{\text{base}}$ is the base leaner loss. The prediction on the j^{th} query sample for task T is then given by $b_{\theta^*}(m_{\phi}(\tilde{x}_j))$. In contrast to the task-specific base learner, the meta learner \mathcal{M} trains a general model aiming to perform well on many, if not all tasks. \mathcal{M} learns a generalized meta network m_{ϕ}^* over T . The meta-learning phase can be written as,

$$\mathcal{M}(D) := \phi^* = \arg \min_{\phi} \mathbb{E}_{T \sim \mathcal{T}} \mathcal{L}_{\text{meta}}(T, m_{\phi}; b_{\theta^*}), \quad (2)$$

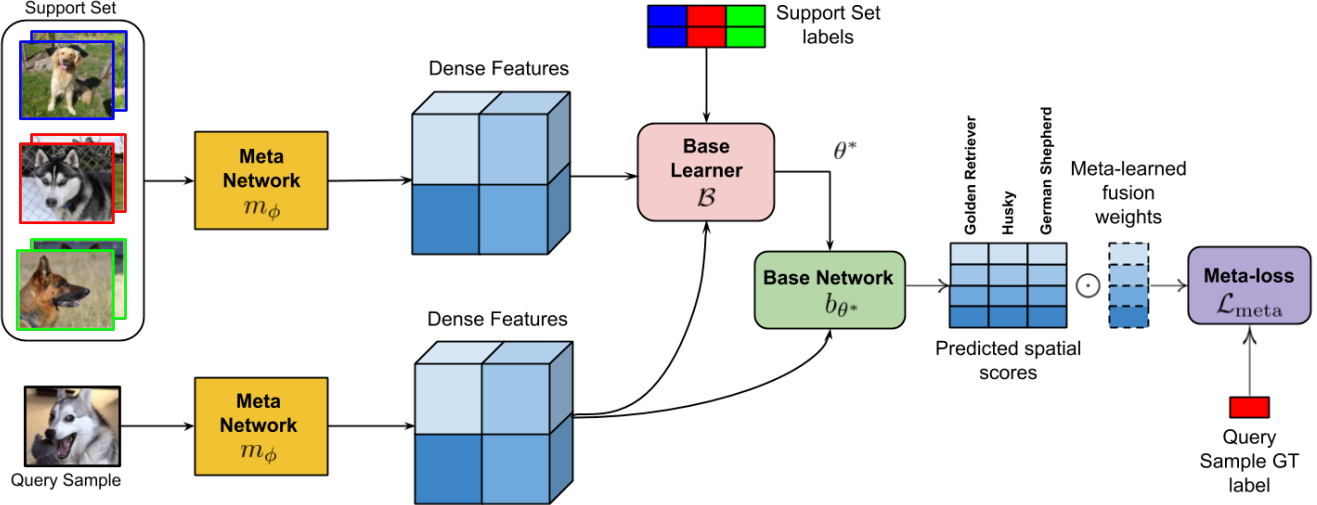


Figure 1: Overview of FIML (Few-Iteration Meta-Learning) for a 3-way 2-shot classification task.

where \mathcal{T} is a set of k -way, n -shot classification problems sampled from D and $\mathcal{L}_{\text{meta}}$ is the meta loss. The aim for the meta learner \mathcal{M} is thus to learn a rich feature representation m_{ϕ^*} over which the base learner \mathcal{B} can learn to classify the query samples. The training process mimics what happens during inference, except that the meta network m_{ϕ^*} remains fixed and only the base network b_{θ} is learned according to the given task T shown to the base learner \mathcal{B} . Our base learner consists of an inductive objective, a transductive objective, and an optimization method, presented in the following sections. Fig. 3 visualizes our approach.

3.2. Inductive Objective

In this section, we describe the task-specific base network b_{θ} and the base learner \mathcal{B} . Given a task T , our aim is to learn a classifier b_{θ} , taking the representation learned by the meta-network as input. For an image x , the base network predicts classification scores $b_{\theta}(m_{\phi}(x)) \in \mathbb{R}^k$ for each of the k classes. The base learner \mathcal{B} minimizes $\mathcal{L}_{\text{base}}$ w.r.t. the parameters θ . To this end, we start from a least squares objective as it allows effective optimization, which is crucial for practical meta-learning. In general, we consider a base learner objective of the following form,

$$\mathcal{L}_{\text{ind}}(\theta) = \sum_{j=1}^N \|r(b_{\theta}(m_{\phi}(x_j)), \delta_{y_j})\|^2. \quad (3)$$

Here, r is a general residual error function and $\delta_{y_j} \in \mathbb{R}^k$ is a one-hot representation of the label y_j .

The most straightforward choice for the residual function is to simply take the difference $r(s, \delta_y) = s - \delta_y$. For a linear base network b_{θ} , this leads to a linear least squares

ridge regression problem, as previously considered in a meta-learning context [1]. However, such a loss is not a robust choice in the classification setting, since it penalizes any deviation from the target value δ_y . In particular, *easy* samples, residing on the correct side of the classification boundary, often dominate over *hard* samples. This issue is classically addressed by the SVM model, adopted by MetaOptNet [15], employing the hinge loss to ignore easy samples.

We take inspiration from the hinge loss, but propose a learnable parametrized alternative, suitable for the least-squares setting (13). Our residual function is defined as,

$$r(s_j, \delta_{y_j}) = \max(z_j \cdot (l_j - s_j), a_j \cdot z_j \cdot (l_j - s_j)), \quad (4)$$

where $z_j = 2\delta_{y_j} - 1$ signifies whether the class is positive or negative and $l_j = l_+ \delta_{y_j} + l_- (1 - \delta_{y_j})$ is the modified ground truth regression target with l_+ and l_- being the target regression scores for the positive and negative classes, respectively. And, the predicted scores $s_j = b_{\theta}(x_j)$. Intuitively, the parameters l_+ and l_- define the margins of the classifier for the positive and the negative classes, respectively. The parameter $a_j = a_+ \delta_{y_j} + a_- (1 - \delta_{y_j})$, where a_+ and a_- are the coefficient of leakage for the positive and negative classes respectively. The coefficients of leakage (a_+ and a_-) and the target regression scores (l_+ and l_-) are the free parameters in our base loss formulation which makes our loss more adaptive and robust at the same time. The free parameters of the loss are learned by the meta learner \mathcal{M} during meta-training. Lastly, we note that although the max operation in (4) is not continuously differentiable, there are smooth alternatives, *e.g.* the log-sum-exp function, that well approximates its behaviour.

3.3. Transductive Objective

Base learner modules for few-shot learning algorithms often suffer from high variance due to the low amount of labeled data available. However, the base learner \mathcal{B} also has access to the unlabeled query samples, often ignored by meta-learning methods. These can aid the base learner by constraining the hypothesis search space. This setting is very similar to a semi-supervised learning setup [14, 19]. Recent metric-learning based few-shot classification methods [9, 17] have demonstrated encouraging results by integrating transductive strategies. Instead, we propose a strategy for integrating transductive learning into optimization-based meta-learning. Our approach is formulated as a regularization, inspired by work [8] from the semi-supervised learning literature.

Although the base learner does not know to which class a query sample belongs, there is an important piece of information that it can exploit. Namely, that the query sample belongs to exactly *one* of the categories in the task. This introduces a constraint, that can be formulated as an objective. In this work, we penalize the Shannon Entropy of the predictions on the query samples, stimulating the base learner to find classification parameters that yield confident predictions on the query set. Our transductive term is given by,

$$\begin{aligned}\mathcal{L}_{\text{tran}}(\theta) &= - \sum_{j=1}^{\tilde{N}} \sum_{c=1}^k \tilde{p}_j^c \log \tilde{p}_j^c \\ &= \sum_{j=1}^{\tilde{N}} \left(\log \sum_{c=1}^k e^{\tilde{s}_j^c} - \frac{\sum_{c=1}^k \tilde{s}_j^c e^{\tilde{s}_j^c}}{\sum_{c=1}^k e^{\tilde{s}_j^c}} \right).\end{aligned}\quad (5)$$

Here, $\tilde{s}_j = \beta b_\theta(m_\phi(\tilde{x}_j))$, \tilde{x}_j is the j^{th} query sample and \tilde{s}_j^c is its logit for class c . The second equality simply follows from the substitution of $\tilde{p}_j = \text{SoftMax}(\tilde{s}_j)$. Note that we have introduced a temperature scaling parameter β . By learning this parameter during meta-training, our approach learns to calibrate the query classification probabilities in order to benefit the transductive learning. Our final base learner objective, integrating both the inductive (13) and the transductive (14) terms is thus,

$$\mathcal{L}_{\text{base}}(\theta) = \mathcal{L}_{\text{ind}}(\theta) + \lambda_{\text{tran}} \mathcal{L}_{\text{tran}}(\theta) + \lambda_{\text{reg}} \|\theta\|^2. \quad (6)$$

The second term is a regularization on the base learned parameters θ . Since the objective (15) is utilized in the base learner, we can even learn the importance weights λ_{tran} and λ_{reg} during meta-training, thus circumventing the need for tuning by hand. Next, we derive our base learner $\theta^* = \mathcal{B}(T; m_\phi)$ by applying an unrolled optimization procedure to minimize (15).

3.4. Base Learner Optimization

Our base learner (1) is implemented by applying an iterative optimization algorithm to our objective (15). Meta-

learning methods popularly resort to the standard gradient descent algorithm [6]. However, we primarily consider a linear base model $b_\theta(x) = \theta x$, where θ are the linear classification weights, allowing more effective strategies that enjoy substantially faster convergence to be employed. We therefore adapt the Steepest Descent based strategy [2] to our setting.

We start from a positive definite quadratic approximation of the objective (15). Although our objective is non-convex, such an approximation can be derived using Gauss-Newton for (13) and a positive definite approximate Hessian of (14). We provide a detailed derivation in the appendix. The quadratic approximation provides the optimal step length $\alpha^{(d)}$ in the gradient direction through a simple closed-form expression. The optimization iteration is expressed as,

$$\begin{aligned}\theta^{(d+1)} &= \theta^{(d)} - \alpha^{(d)} \nabla \mathcal{L}_{\text{base}}(\theta^{(d)}) \text{ where,} \\ \alpha^{(d)} &= \frac{\nabla \mathcal{L}_{\text{base}}(\theta^{(d)})^T \nabla \mathcal{L}_{\text{base}}(\theta^{(d)})}{\nabla \mathcal{L}_{\text{base}}(\theta^{(d)})^T H^{(d)} \nabla \mathcal{L}_{\text{base}}(\theta^{(d)})}.\end{aligned}\quad (7)$$

Here, d denotes the iteration number. Note that the positive definite Hessian approximation $H^{(d)}$ does not need to be computed explicitly. Instead, both the computation of the gradient $\nabla \mathcal{L}_{\text{base}}$ and the Hessian-gradient product $H^{(d)} \nabla \mathcal{L}_{\text{base}}$ can be efficiently implemented using standard network operations or double-backpropagation (see appendix).

To further reduce the number of required iterations in (17), we propose an effective initialization strategy to obtain $\theta^{(0)}$. We express the initial classification weights $\theta_c^{(0)}$ of class c as a linear combination between the average positive f_{pos}^c and negative f_{neg}^c feature vectors in the support set,

$$\begin{aligned}\theta_c^{(0)} &= \kappa^c f_{\text{pos}}^c - \tau^c f_{\text{neg}}^c \text{ where,} \\ f_{\text{pos}}^c &= \frac{1}{n} \sum_{j=1}^N \mathbb{1}_{y_j=c} m_\phi(x_j) \text{ and,} \\ f_{\text{neg}}^c &= \frac{1}{N-n} \sum_{j=1}^N \mathbb{1}_{y_j \neq c} m_\phi(x_j).\end{aligned}\quad (8)$$

Here, N is the number of samples in the support set S for task T for an n -shot problem. The two scalars $\kappa^c, \tau^c \in \mathbb{R}$ are found by defining two linear constraints $(f_{\text{pos}}^c)^T \theta_c^{(0)} = o_+$ and $(f_{\text{neg}}^c)^T \theta_c^{(0)} = o_-$ and are given by:

$$\kappa = \frac{o_+ \cdot f_{\text{neg}}^c {}^T f_{\text{neg}}^c - o_- \cdot f_{\text{pos}}^c {}^T f_{\text{neg}}^c}{f_{\text{pos}}^c {}^T f_{\text{pos}}^c \cdot f_{\text{neg}}^c {}^T f_{\text{neg}}^c - (f_{\text{pos}}^c {}^T f_{\text{neg}}^c)^2} \quad (9)$$

$$\tau = \frac{o_+ \cdot f_{\text{pos}}^c {}^T f_{\text{neg}}^c - o_- \cdot f_{\text{pos}}^c {}^T f_{\text{pos}}^c}{f_{\text{pos}}^c {}^T f_{\text{pos}}^c \cdot f_{\text{neg}}^c {}^T f_{\text{neg}}^c - (f_{\text{pos}}^c {}^T f_{\text{neg}}^c)^2}. \quad (10)$$

Here o_+, o_- represent the classification score for f_{pos}^c and f_{neg}^c . We learn the values of o_+, o_- during meta-training. Un-

like Proto-MAML [29] which initializes the task-specific linear layer with the Prototypical Network-equivalent weights, our base learner initializer also aims to exploit the negative examples which increases the discriminative ability.

3.5. Dense Classification

In this section, we further address the scarcity of labeled data by integrating a dense classification strategy, utilizing samples extracted from different spatial locations in the image. Recently, Lifchitz *et al.* [16] demonstrated the benefit of using dense features for few-shot classification tasks. Standard deep embedding networks m_ϕ terminate with a global average pooling layer. This leads to a loss of information that could prove detrimental to the performance of few-shot classification algorithms. We, therefore, utilize dense spatial features before the global average pooling layer in m_ϕ . Let $m_\phi^l(x)$ be the feature vector at spatial index l . Our previously described base learner is modified to operate on these localized features by simply treating them as individual examples in the support and query sets, respectively. Both, our inductive (13) and transductive (14) objectives thus includes one term per spatial location in the dense feature map obtained from m_ϕ . While this strategy allows us to learn from multiple localized examples, our task is to generate one final prediction per query image. This is achieved through a spatial fusion procedure,

$$\tilde{s}_j = \sum_l v_l b_{\theta^*} (m_\phi^l(\tilde{x}_j)) , \quad (11)$$

where $\{v_l\}_l$ is a set of spatial weights that are learned during meta-training. These weights signify how much emphasis must be given to a prediction of the base network b_{θ^*} for a certain spatial location.

The fused scores (11) serve as the logits for the final classification output. During meta-training, we minimize the cross-entropy to the ground-truth probability vector \hat{p}_j for each query sample \tilde{x}_j in the task as,

$$\mathcal{L}_{\text{meta}}(\phi, \psi) = -\frac{1}{\tilde{N}} \sum_{j=1}^{\tilde{N}} \sum_{c=1}^k \hat{p}_j^c \log \tilde{p}_j^c. \quad (12)$$

Here $\tilde{p}_j = \text{SoftMax}(\tilde{s}_j)$. In addition to the parameters ϕ of the embedding network, we meta-learn parameters of our base-learner $\psi = \{l_+, l_-, a_+, a_-, \beta, \lambda_{\text{tran}}, \lambda_{\text{reg}}, o_+, o_-, \{v_l\}_l\}$. The latter include parameters of our inductive and transductive objectives, along with the optimization parameters and the fusion weights.

4. Experiments

4.1. Implementation Details

We implement our approach using PyTorch [21]. Our experiments are conducted with two different embedding

networks m_ϕ commonly used for few-shot classification, namely ResNet-12 and WideResNet-28-10. Both the backbones are trained from scratch during meta-training. We follow the meta-training and meta-testing strategies used in [15]. As an optimizer, we use SGD [3] with Nesterov momentum of 0.9 and weight decay of 0.0005. We meta-train the model for 60 epochs, each containing 1000 batches. Each batch consists of 16 tasks. The number of iterations for base network optimizer at train time was set to 10 during meta-training and 15 during meta-testing. At training time, the best model is chosen based on 5-way, n -shot classification accuracy on the validation set. Following [15], the network is first trained using a 15-shot setting. Since we aim to learn the base learner itself for a particular distribution of tasks, we further fine-tune the base learner parameters ψ in (12) for 10 epochs for the specific shot setting using a learning rate of 0.001. Code and trained models will be released upon publication. Now, we give a brief overview of the few-shot classification benchmarks, which we use for evaluating our approach. Training was performed on four NVIDIA Tesla V100 GPUs.

4.2. Few-shot Classification Benchmarks

ImageNet Derivatives: The miniImageNet [23] and the tieredImageNet [24] few-shot classification benchmarks are derived from ILSVRC-2012 [25]. While miniImageNet consists of 100 randomly sampled classes from ILSVRC-2012, tieredImageNet is a larger subset of ILSVRC-2012, which consists of a class hierarchy and comprises of images from 34 superclasses of ILSVRC-2012. The image size in both the benchmarks is 84×84 . The train, validation, and test splits for the miniImageNet dataset comprise of samples from 64, 16, and 20 classes, respectively. Conversely, to minimize semantic similarity between the splits, tieredImageNet splits data based on the superclasses. The train, validation, and test splits for the consists of images from 20, 6, and 8 superclasses, respectively.

CIFAR-100 Derivatives: Both, the CIFAR-FS [1] and the FC100 [20] benchmarks encompass the full CIFAR-100 dataset [12]. The difference lies only in the split scheme for both the datasets. While the CIFAR-100 dataset is split based on the subclasses to derive the CIFAR-FS dataset; FC100, similar to tieredImageNet, splits CIFAR-100 based on superclasses to minimize semantic similarity. For CIFAR-FS, the classes are randomly split into 64, 16, and 20 for training, validation, and testing, respectively. Whereas, for FC100, the train, validation, and test splits contain data from 12, 4, and 4 CIFAR-100 superclasses, respectively. The image size is 32×32 in both the datasets.

4.3. Ablation Study

We perform an ablative study on the two larger few-shot classification datasets, namely the miniImageNet and tiered-

Table 1: Ablative study of our approach on tieredImageNet and miniImageNet datasets. Results are reported in terms of accuracy (%) with 95% confidence interval.

	miniImageNet 5-way		tieredImageNet 5-way	
	1-shot	5-shot	1-shot	5-shot
Baseline	64.73 \pm 0.73	80.89 \pm 0.54	61.97 \pm 0.69	78.12 \pm 0.48
+Initializer	65.32 \pm 0.71	81.06 \pm 0.57	62.13 \pm 0.68	78.56 \pm 0.45
+Dense Features	66.41 \pm 0.64	82.96 \pm 0.51	63.01 \pm 0.64	79.45 \pm 0.44
+LearnLoss	67.27 \pm 0.66	83.83 \pm 0.52	63.67 \pm 0.65	80.17 \pm 0.46
+Transductive	69.92 \pm 0.64	84.41 \pm 0.55	65.00 \pm 0.64	80.52 \pm 0.43

ImageNet. The methods are compared in terms of the few-shot classification accuracy (%) with a 95% confidence interval. Results are reported in Tab. 9.

Baseline: As the baseline, we meta-train and meta-test our framework with fixed hyperparameters ($l_+ = 1$, $l_- = -1$, $a_+ = 1$, $a_- = 1$ in 4 and $\lambda_{\text{reg}} = 0.01$ in (15)). Note that this configuration implies a linear ridge regression objective, similar to [1]. Further we use a zero initializer $\theta^{(0)} = 0$ in our base learner (Sec. 3.4). We do not include the transductive objective ($\lambda_{\text{tran}} = 0$) and do not use the dense classification strategy described in Sec. 3.5.

+Initializer: This version adds the support set based initialization of $\theta^{(0)}$ discussed in section 3.4 to the baseline. The parameters o_+ and o_- are fixed to the fixed value 1. **+Initializer** improves over the baseline with a relative gain of 0.9% for 1-shot evaluation on the tieredImageNet dataset. This ablation suggests that our base network initializer leads to a faster convergence for the base learner.

+DenseFeatures: Next, we investigate the effect of using the spatial dense classification strategy, discussed in Sec. 3.5, by adding it to the previous configuration. In this version, we keep the spatial fusion weights fixed along with the other base learner parameters. Specifically, we use an average pooling of logits in (11) by setting $v_l = 1/L$, where L is the number of spatial feature locations. The utilization of dense features leads to a significant increase in the performance over +IntelInit, with relative gains of 1.7% and 2.3% for 1-shot and 5-shot performance, respectively, on tieredImageNet.

+LearnLoss: Here, we additionally learn all the parameters ψ of the base learner, defined in Sec. 3.5. These include the parameters of the inductive loss, optimizer, and the spatial fusion weights for dense classification. By exploiting the flexibility of our framework to learn the optimal base learner through meta-training, **+LearnLoss** achieves a substantial relative increment of 1.3% and 1.0% for 1-shot and 5-shot performance on tieredImageNet. Results on miniImageNet follow a similar trend, with relative improvements of 1% and 0.9% for 1-shot and 5-shot respectively.

+Transductive: Finally, we add the transductive term 14 to our overall objective (15). The free parameters of

Table 2: Analysis of the number of optimization steps for the base learner at train time on 1-shot and 5-shot test accuracies (%) with 95% confidence intervals for tieredImageNet. The number of iteration at test time are fixed to 15.

	Number of iterations			
	0	5	10	15
1-shot	65.01 \pm 0.70	68.73 \pm 0.66	69.92 \pm 0.64	69.56 \pm 0.68
5-shot	81.32 \pm 0.58	83.14 \pm 0.54	84.41 \pm 0.55	83.82 \pm 0.54

the transductive term, *i.e.* the importance weight λ_{tran} and the temperature scaling β are learned by the meta-learner. Adding the transductive loss for learning an optimal base network gives a major improvement in 1-shot performance, with relative gains of 3.9% and 2.1% for tieredImageNet and miniImageNet, respectively. The improvement in the 5-shot setting is more modest, but still significant. The results follow an expected trend, since the potential benefit of transductive learning increases when the number of labeled examples are reduced. Interestingly, a more detailed investigation showed that the learned importance weight λ_{tran} for the transductive objective was substantially larger in the 1-shot scenario compared to when trained for the 5-shot setting. This demonstrates that our approach is capable of meta-learning not only the feature embedding, but also the base learner itself. We use this version of our approach for the state-of-the-art comparisons presented in Sec. 4.4.

Number of iterations: Next, we analyze the effect of the number of steepest descent optimization iterations used within the base learner. Fig. 2 plots the 5-way 1-shot and

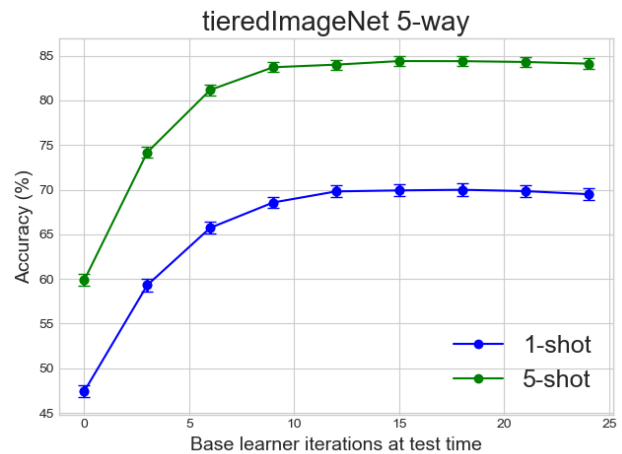


Figure 2: Analysis of the number of optimization steps for the base learner at test time on 1-shot and 5-shot test accuracy (%) with 95% confidence interval for tieredImageNet. The number of iteration at train time are fixed to 10.

Table 3: Cross-validation across datasets (WRN-28-10 backbone) for a 5-way task.

		FIML	FIML-CrossVal
tieredImageNet	1-shot	72.97 \pm 0.47	73.06 \pm 0.50
	5-shot	86.12 \pm 0.37	85.90 \pm 0.41
miniImageNet	1-shot	67.89 \pm 0.42	67.95 \pm 0.39
	5-shot	82.31 \pm 0.33	82.46 \pm 0.35
FC100	1-shot	45.01 \pm 0.46	44.91 \pm 0.44
	5-shot	58.96 \pm 0.51	59.27 \pm 0.54
CIFAR-FS	1-shot	77.21 \pm 0.46	77.08 \pm 0.41
	5-shot	88.49 \pm 0.33	88.70 \pm 0.36

5-shot test accuracy on tieredImageNet w.r.t. the number of iterations used during inference. This is performed on our final model, which uses 10 iterations during meta-training. The performance saturates at about 15 inference iterations. For a larger, we observe a slight tendency of overfitting. In Tab. 8 we instead vary the number of iterations employed during meta-training, while employing a fixed number of 15 iterations during inference. The results improve by increasing the number of iterations during meta-training. This clearly demonstrates that our base learner does not simply act as a fine-tuning mechanism, but significantly benefits the meta-learning process.

Cross-validation across datasets: Learning the loss parameters ψ on a single dataset can lead to overfitting. To analyze potential dataset-specific overfitting, we perform cross-validation of the learned loss parameters ψ across datasets (Tab. 3). For reporting the cross-validation accuracies (FIML-CrossVal), we evaluate the model trained for tieredImageNet on FC100 and CIFAR-100. Similarly, we evaluate the ψ parameters trained for FC100 to report accuracies on the datasets derived from miniImageNet. When using the loss parameters ψ learned on tieredImageNet, the average classification accuracy only changes by 0.10% and 0.31% for 1-shot and 5-shot, respectively on the FC100 dataset, while the opposite leads to a change of 0.09% and 0.22% on the tieredImageNet dataset, respectively. The learned loss thus generalizes well to other datasets yielding comparable performances to FIML in all cases.

Additional ablation studies are provided in the Appendix.

4.4. State-of-the-Art

We compare our approach FIML with state-of-the-art methods for few-shot classification. In Tab. 4 we report results on miniImageNet and tieredImageNet, while Tab. 5 shows results for CIFAR-FS and FC100. Among the compared methods, R2D2 [1] and MetaOptNet-SVM [15] employ an optimization-based base learner that predicts the parameters of a linear classification head. Our approach

significantly outperforms these methods. Notably, when employing the same ResNet-12 backbone, our approach achieves relative improvements of 3.6% and 2.4% for 1-shot and 5-shot performance, respectively, on the larger tieredImageNet dataset. Moreover, compared to MetaOptNet-SVM [15] and R2D2 [1], our framework can utilize a wider class of objective functions, allowing us to integrate the non-convex transductive objective (14) and also to meta-learn important parameters of the objective and the base learner itself. We also implemented a dense classification version of MetaOptNet-SVM (MetaOptNet-SVM+Dense), but did not find it to yield any significant improvement. We also compare the computational time of FIML and MetaOptNet+Dense on tieredImageNet. For MetaOptNet+Dense, the number of QP solver iterations were carefully set based on the validation set for the best test accuracy, whereas the standard setting of 15 iterations were run for the base learner optimizer to time FIML. Tab. 6 shows the timings in milliseconds (ms) per episode for 1-shot, 5-shot and 15-shot tasks. It is evident that FIML scales better than MetaOptNet+Dense w.r.t. the number of shots during inference. Among other compared methods, DC [17] and CAN [9] utilize dense classification. The latter is a recent metric-learning based method, employing pairwise cross attention maps for the class prototypes and the query samples for extracting discriminative features. Further, CAN+Transduction augment the support set with the query samples to learn more representative class prototypes. The query samples are assigned to a particular class based on the nearest neighbors of the query sample in the support set. This approach achieves strong performance, particularly for the 1-shot case. While our work is the first to integrate transductive strategies into an optimization-based meta-learning framework, the results of CAN show that there is scope for further improvements in this direction. When using the WideResNet backbone, our approach significantly improves over CAN+Transduction in the 5-shot setting, while achieving similar or better for 1-shot. Our strong iterative base-learner on top of a discriminative embedding network as in CAN [9] could provide a significant boost in performance. Unfortunately, we cannot test this since the code for [9] has not been released.

Lastly, we compare our approach with the very recent method Trans-FT [5]. This approach does not perform meta-learning, but directly addresses the few-shot learning problem by learning a generalizable representation using the class labels in the training set. Given the learned representation, the few-shot classifier is trained during testing, using both, a inductive classification loss and a transductive loss. On tieredImageNet, our method improves on Trans-FT in the 5-shot case, with a slight degradation in 1-shot performance. However, our approach outperforms Trans-FT on all other datasets, achieving relative gains of 3.3% and 5% for 1-shot and 5-shot evaluations, respectively, on miniImageNet. Fur-

Table 4: Few-shot classification accuracy (%) with 95% confidence intervals on meta-test splits. 4-layer convolutional networks are represented as a sequence denoting the number of filters in each layer.

Method	Backbone	miniImageNet 5-way		tieredImageNet 5-way	
		1-shot	5-shot	1-shot	5-shot
CAVIA [31]	32-32-32-32	47.24 \pm 0.65	59.05 \pm 0.54	-	-
MAML [6]	32-32-32-32	48.70 \pm 1.84	63.11 \pm 0.92	51.67 \pm 1.81	70.30 \pm 1.75
Matching Networks [30]	64-64-64-64	43.56 \pm 0.84	55.31 \pm 0.73	-	-
Relation Networks [28]	64-96-128-256	50.44 \pm 0.82	65.32 \pm 0.70	54.48 \pm 0.93	71.32 \pm 0.78
LSTM Meta Learner [23]	64-64-64-64	43.44 \pm 0.77	60.60 \pm 0.71	-	-
Transductive Propagation [17]	64-64-64-64	55.51 \pm 0.86	69.86 \pm 0.65	59.91 \pm 0.49	73.30 \pm 0.45
R2D2 [1]	96-192-384-512	51.20 \pm 0.60	68.80 \pm 0.10	-	-
TADAM [20]	ResNet-12	58.50 \pm 0.30	76.70 \pm 0.30	-	-
MetaOptNet-SVM [15]	ResNet-12	62.64 \pm 0.61	78.63 \pm 0.46	65.99 \pm 0.72	81.56 \pm 0.53
MetaOptNet-SVM [15]+Dense	ResNet-12	61.69 \pm 0.55	79.13\pm0.43	65.17 \pm 0.67	81.44 \pm 0.45
DC [17]	ResNet-12	61.26 \pm 0.20	79.01 \pm 0.13	-	-
CAN [9]	ResNet-12	63.85 \pm 0.48	79.44\pm0.34	69.89\pm0.51	84.23\pm0.37
CAN+Transduction [9]	ResNet-12	67.19\pm0.55	80.64\pm0.35	73.21\pm0.58	84.93\pm0.38
FIML (Ours)	ResNet-12	65.00\pm0.64	80.52\pm0.43	69.92\pm0.64	84.41\pm0.55
LEO [26]	WideResNet-28-10	61.76 \pm 0.08	77.59 \pm 0.12	66.33 \pm 0.05	81.44 \pm 0.09
Trans-FT [5]	WideResNet-28-10	65.73\pm0.78	78.40\pm0.52	73.34\pm0.71	85.50\pm0.50
FIML (Ours)	WideResNet-28-10	67.89\pm0.42	82.31\pm0.33	72.97\pm0.47	86.12\pm0.37

Table 5: Few-shot classification accuracy (%) with 95% confidence intervals on meta-test splits. 4-layer convolutional networks are represented as a sequence denoting the number of filters in each layer.

Method	Backbone	CIFAR-FS 5-way		FC100 5-way	
		1-shot	5-shot	1-shot	5-shot
Relation Networks [28]	64-96-128-256	55.00 \pm 1.00	69.30 \pm 0.80	-	-
MAML [6]	32-32-32-32	58.90 \pm 1.90	71.50 \pm 1.00	-	-
R2D2 [1]	96-192-384-512	65.30 \pm 0.20	79.40 \pm 0.10	-	-
Prototypical Networks [27]	ResNet-12	72.20 \pm 0.70	83.50 \pm 0.50	37.50 \pm 0.60	52.50 \pm 0.60
TADAM [20]	ResNet-12	-	-	40.10 \pm 0.40	56.10 \pm 0.40
MetaOptNet-SVM [15]	ResNet-12	72.00 \pm 0.70	84.20\pm0.50	41.10 \pm 0.60	55.50 \pm 0.60
MetaOptNet-SVM [15]+Dense	ResNet-12	72.23\pm0.65	83.65 \pm 0.47	41.56 \pm 0.59	55.97 \pm 0.55
DC [16]	ResNet-12	-	-	42.04\pm0.17	57.05\pm0.16
FIML (Ours)	ResNet-12	75.13\pm0.66	85.61\pm0.44	42.75\pm0.56	57.23\pm0.54
Trans-FT [5]	WideResNet-28-10	76.58 \pm 0.68	85.79 \pm 0.50	43.16 \pm 0.59	57.57 \pm 0.55
FIML (Ours)	WideResNet-28-10	77.21\pm0.46	88.49\pm0.33	45.01\pm0.46	58.96\pm0.51

Table 6: Comparison of mean inference times (in ms) with 95% confidence interval of FIML with MetaOptNet-SVM (with dense features) and Trans-FT on the tieredImageNet dataset for a 5-way task.

		1-shot	5-shot	15-shot
ResNet-12	MetaOptNet-SVM [15]+Dense	79 \pm 15	109 \pm 20	174 \pm 16
	FIML (ours)	67 \pm 18	91 \pm 17	133 \pm 21
WideResNet-28-10	Trans-FT [5]	20800	-	-
	FIML (ours)	107 \pm 24	159 \pm 30	261 \pm 28

ther, a major disadvantage of [5] is its computational complexity. In fact, our approach is about 200 \times faster (Tab. 9): 20.8s is reported in [5] while we achieve 0.107 \pm 0.024s in the same setting (one 1-shot, 5-way, task with 15 queries) and backbone (WideResNet-28-10). Runtime is of crucial importance in applications involving learning agents and other time-critical systems. This indicates the advantage of meta-learning based methods. Further, in contrast to the manual hand-tuning required in [5], our approach automatically learns the crucial hyper-parameters associated with the few-shot objective, including the temperature scaling and

the balance between the losses.

5. Conclusion

We propose an iterative optimization-based meta-learning method FIML, which integrates dense features with a novel adaptive fusion module in a few-shot setting. FIML consists of a base-learner, employing a robust classification loss. A transductive loss term is also integrated into our flexible framework, forcing the base network to make confident predictions on the query samples. Further, a support set based initialization of the linear base network aids the iterative unrolled optimizer in a faster convergence of the base network. We experimentally validate our approach on four few-shot classification benchmarks and set a new state-of-the-art for optimization-based meta-learning.

6. Acknowledgement

This work was supported by the ETH Zurich Fund (OK), a Huawei Technologies Oy (Finland) project, an Amazon AWS grant, and a Nvidia GPU grant.

References

- [1] Luca Bertinetto, João F. Henriques, Philip H. S. Torr, and Andrea Vedaldi. Meta-learning with differentiable closed-form solvers. In *7th International Conference on Learning Representations, ICLR 2019, New Orleans, LA, USA, May 6-9, 2019*. OpenReview.net, 2019.
- [2] Goutam Bhat, Martin Danelljan, Luc Van Gool, and Radu Timofte. Learning discriminative model prediction for tracking. In *Proceedings of the IEEE International Conference on Computer Vision*, pages 6182–6191, 2019.
- [3] Léon Bottou and Olivier Bousquet. The tradeoffs of large scale learning. In *Advances in neural information processing systems*, pages 161–168, 2008.
- [4] Wei-Yu Chen, Yen-Cheng Liu, Zsolt Kira, Yu-Chiang Frank Wang, and Jia-Bin Huang. A closer look at few-shot classification. In *7th International Conference on Learning Representations, ICLR 2019, New Orleans, LA, USA, May 6-9, 2019*. OpenReview.net, 2019.
- [5] Guneet Singh Dhillon, Pratik Chaudhari, Avinash Ravichandran, and Stefano Soatto. A baseline for few-shot image classification. In *8th International Conference on Learning Representations, ICLR 2020, Addis Ababa, Ethiopia, April 26-30, 2020*. OpenReview.net, 2020.
- [6] Chelsea Finn, Pieter Abbeel, and Sergey Levine. Model-agnostic meta-learning for fast adaptation of deep networks. In *Proceedings of the 34th International Conference on Machine Learning-Volume 70*, pages 1126–1135. JMLR.org, 2017.
- [7] Victor Garcia and Joan Bruna. Few-shot learning with graph neural networks. *arXiv preprint arXiv:1711.04043*, 2017.
- [8] Yves Grandvalet and Yoshua Bengio. Semi-supervised learning by entropy minimization. In *Advances in neural information processing systems*, pages 529–536, 2005.
- [9] Ruibing Hou, Hong Chang, MA Bingpeng, Shiguang Shan, and Xilin Chen. Cross attention network for few-shot classification. In *Advances in Neural Information Processing Systems*, pages 4005–4016, 2019.
- [10] Jongmin Kim, Taesup Kim, Sungwoong Kim, and Chang D. Yoo. Edge-labeling graph neural network for few-shot learning. In *IEEE Conference on Computer Vision and Pattern Recognition, CVPR 2019, Long Beach, CA, USA, June 16-20, 2019*, pages 11–20. Computer Vision Foundation / IEEE, 2019.
- [11] Gregory Koch, Richard Zemel, and Ruslan Salakhutdinov. Siamese neural networks for one-shot image recognition. In *ICML deep learning workshop*, volume 2. Lille, 2015.
- [12] Alex Krizhevsky, Vinod Nair, and Geoffrey Hinton. Cifar-10 and cifar-100 datasets. URL: <https://www.cs.toronto.edu/~kriz/cifar.html>, 6, 2009.
- [13] Brenden M Lake, Ruslan Salakhutdinov, and Joshua B Tenenbaum. Human-level concept learning through probabilistic program induction. *Science*, 350(6266):1332–1338, 2015.
- [14] Dong-Hyun Lee. Pseudo-label: The simple and efficient semi-supervised learning method for deep neural networks. In *Workshop on challenges in representation learning, ICML*, volume 3, page 2, 2013.
- [15] Kwonjoon Lee, Subhransu Maji, Avinash Ravichandran, and Stefano Soatto. Meta-learning with differentiable convex optimization. In *Proceedings of the IEEE Conference on Computer Vision and Pattern Recognition*, pages 10657–10665, 2019.
- [16] Yann Lifchitz, Yannis Avrithis, Sylvaine Picard, and Andrei Bursuc. Dense classification and implanting for few-shot learning. In *Proceedings of the IEEE Conference on Computer Vision and Pattern Recognition*, pages 9258–9267, 2019.
- [17] Yanbin Liu, Juho Lee, Minseop Park, Saehoon Kim, Eunho Yang, Sung Ju Hwang, and Yi Yang. Learning to propagate labels: Transductive propagation network for few-shot learning. In *7th International Conference on Learning Representations, ICLR 2019, New Orleans, LA, USA, May 6-9, 2019*. OpenReview.net, 2019.
- [18] Alex Nichol, Joshua Achiam, and John Schulman. On first-order meta-learning algorithms. *CoRR*, abs/1803.02999, 2018.
- [19] Avital Oliver, Augustus Odena, Colin A Raffel, Ekin Dogus Cubuk, and Ian Goodfellow. Realistic evaluation of deep semi-supervised learning algorithms. In *Advances in Neural Information Processing Systems*, pages 3235–3246, 2018.
- [20] Boris Oreshkin, Pau Rodríguez López, and Alexandre Lacoste. Tadam: Task dependent adaptive metric for improved few-shot learning. In *Advances in Neural Information Processing Systems*, pages 721–731, 2018.
- [21] Adam Paszke, Sam Gross, Soumith Chintala, Gregory Chanan, Edward Yang, Zachary DeVito, Zeming Lin, Alban Desmaison, Luca Antiga, and Adam Lerer. Automatic differentiation in pytorch. 2017.
- [22] Aravind Rajeswaran, Chelsea Finn, Sham M. Kakade, and Sergey Levine. Meta-learning with implicit gradients. In Hanna M. Wallach, Hugo Larochelle, Alina Beygelzimer,

Florence d’Alché-Buc, Emily B. Fox, and Roman Garnett, editors, *Advances in Neural Information Processing Systems 32: Annual Conference on Neural Information Processing Systems 2019, NeurIPS 2019, 8-14 December 2019, Vancouver, BC, Canada*, pages 113–124, 2019.

[23] Sachin Ravi and Hugo Larochelle. Optimization as a model for few-shot learning. In *5th International Conference on Learning Representations, ICLR 2017, Toulon, France, April 24-26, 2017, Conference Track Proceedings*. OpenReview.net, 2017.

[24] Mengye Ren, Eleni Triantafillou, Sachin Ravi, Jake Snell, Kevin Swersky, Joshua B. Tenenbaum, Hugo Larochelle, and Richard S. Zemel. Meta-learning for semi-supervised few-shot classification. In *6th International Conference on Learning Representations, ICLR 2018, Vancouver, BC, Canada, April 30 - May 3, 2018, Conference Track Proceedings*. OpenReview.net, 2018.

[25] Olga Russakovsky, Jia Deng, Hao Su, Jonathan Krause, Sanjeev Satheesh, Sean Ma, Zhiheng Huang, Andrej Karpathy, Aditya Khosla, Michael Bernstein, et al. Imagenet large scale visual recognition challenge. *International journal of computer vision*, 115(3):211–252, 2015.

[26] Andrei A. Rusu, Dushyant Rao, Jakub Sygnowski, Oriol Vinyals, Razvan Pascanu, Simon Osindero, and Raia Hadsell. Meta-learning with latent embedding optimization. In *7th International Conference on Learning Representations, ICLR 2019, New Orleans, LA, USA, May 6-9, 2019*. OpenReview.net, 2019.

[27] Jake Snell, Kevin Swersky, and Richard Zemel. Prototypical networks for few-shot learning. In *Advances in neural information processing systems*, pages 4077–4087, 2017.

[28] Flood Sung, Yongxin Yang, Li Zhang, Tao Xiang, Philip HS Torr, and Timothy M Hospedales. Learning to compare: Relation network for few-shot learning. In *Proceedings of the IEEE Conference on Computer Vision and Pattern Recognition*, pages 1199–1208, 2018.

[29] Eleni Triantafillou, Tyler Zhu, Vincent Dumoulin, Pascal Lamblin, Utku Evci, Kelvin Xu, Ross Goroshin, Carles Gelada, Kevin Swersky, Pierre-Antoine Manzagol, and Hugo Larochelle. Meta-dataset: A dataset of datasets for learning to learn from few examples. In *International Conference on Learning Representations*, 2020.

[30] Oriol Vinyals, Charles Blundell, Timothy Lillicrap, Daan Wierstra, et al. Matching networks for one shot learning. In *Advances in neural information processing systems*, pages 3630–3638, 2016.

[31] Luisa M. Zintgraf, Kyriacos Shiarlis, Vitaly Kurin, Katja Hofmann, and Shimon Whiteson. Fast context adaptation via meta-learning. In Kamalika Chaudhuri and Ruslan Salakhutdinov, editors, *Proceedings of the 36th International Conference on Machine Learning, ICML 2019, 9-15 June 2019, Long Beach, California, USA*, volume 97 of *Proceedings of Machine Learning Research*, pages 7693–7702. PMLR, 2019.

Appendix

In this appendix, we first provide detailed derivations of the base learner optimization iterations in Sec. A. Sec. B provides an extended study of base learner optimizer iterations at train and test time. In Sec. C, we visualize the effect of the transductive objective in the loss function by plotting bar-charts of the predicted probability scores for the query samples with and without the transductive objective in the loss. Finally, Sec. D provides additional ablations to study the impact of each of our contributions without exploiting the dense features.

A. Closed-form expressions for the base learner optimization

In this section, we provide a derivation for the closed-form solution of the step length α for the optimization iteration (Eq. (7) in the main paper). We first restate the base learner objective terms (Eqs. (3)-(5) in the paper). The inductive objective is given by:

$$\mathcal{L}_{\text{ind}}(\theta) = \sum_{j=1}^N \|r(b_\theta(m_\phi(x_j)), \delta_{y_j})\|^2, \quad (13)$$

where, the residual $r(b_\theta(m_\phi(x_j)), \delta_{y_j})$ is given by Eq. (4) in the main paper. The transductive objective for the base learner is stated as:

$$\mathcal{L}_{\text{tran}}(\theta) = \sum_{j=1}^{\tilde{N}} \left(\log \sum_{c=1}^k e^{\tilde{s}_j^c} - \frac{\sum_{c=1}^k \tilde{s}_j^c e^{\tilde{s}_j^c}}{\sum_{c=1}^k e^{\tilde{s}_j^c}} \right), \quad (14)$$

where, $\tilde{s}_j = \beta b_\theta(m_\phi(\tilde{x}_j))$. Hence, the final base learner objective is given by:

$$\mathcal{L}_{\text{base}}(\theta) = \mathcal{L}_{\text{ind}}(\theta) + \lambda_{\text{tran}} \mathcal{L}_{\text{tran}}(\theta) + \lambda_{\text{reg}} \|\theta\|^2. \quad (15)$$

We start from a positive definite quadratic approximation of the objective (15). This is performed by employing a quadratic approximation of the loss $\mathcal{L}_{\text{base}}$ in the vicinity of the current parameter estimate $\theta^{(d)}$,

$$\begin{aligned} \mathcal{L}_{\text{base}}(\theta) \approx \tilde{\mathcal{L}}_{\text{base}}(\theta) &= \mathcal{L}_{\text{base}}(\theta^{(d)}) + (\theta - \theta^{(d)})^T \nabla \mathcal{L}_{\text{base}}(\theta^{(d)}) \\ &+ \frac{1}{2} (\theta - \theta^{(d)})^T H^{(d)} (\theta - \theta^{(d)}). \end{aligned} \quad (16)$$

Here $H^{(d)}$ is a positive definite Hermitian matrix, detailed below. The Steepest Descent iteration is derived by finding the step length $\alpha^{(d)}$ that minimizes the quadratic approximation (16) in the gradient direction. The iterative formula is then easily expressed as,

$$\begin{aligned} \theta^{(d+1)} &= \theta^{(d)} - \alpha^{(d)} \nabla \mathcal{L}_{\text{base}}(\theta^{(d)}) \text{ where,} \\ \alpha^{(d)} &= \frac{\nabla \mathcal{L}_{\text{base}}(\theta^{(d)})^T \nabla \mathcal{L}_{\text{base}}(\theta^{(d)})}{\nabla \mathcal{L}_{\text{base}}(\theta^{(d)})^T H^{(d)} \nabla \mathcal{L}_{\text{base}}(\theta^{(d)})}. \end{aligned} \quad (17)$$

Here, d denotes the iteration number. Note that the positive definite Hessian approximation $H^{(d)}$ does not need to be computed explicitly. Instead, both the computation of the gradient $\nabla \mathcal{L}_{\text{base}}$ and the Hessian-gradient product $H^{(d)} \nabla \mathcal{L}_{\text{base}}$ can be efficiently implemented using standard network operations. This section elaborates the same.

In order to implement the iterative formula (17), we need an efficient means of computing the gradient $\nabla \mathcal{L}_{\text{base}}$ and find a suitable positive definite Hessian approximation $H^{(d)}$. We first partition the objective $\mathcal{L}_{\text{base}}$ into two terms. The first contains the least squares losses \mathcal{L}_{lsq} , stemming from the inductive \mathcal{L}_{ind} and regularization losses. The second term $\mathcal{L}_{\text{tran}}$ is the transductive loss.

$$\begin{aligned} \mathcal{L}_{\text{base}}(\theta^{(d)}) &= \mathcal{L}_{\text{lsq}}(\theta^{(d)}) + \lambda_{\text{tran}} \mathcal{L}_{\text{tran}}(\theta^{(d)}) \text{ where,} \\ \mathcal{L}_{\text{lsq}}(\theta^{(d)}) &= \mathcal{L}_{\text{ind}}(\theta^{(d)}) + \lambda_{\text{reg}} \|\theta^{(d)}\|^2. \end{aligned} \quad (18)$$

From here on we drop the iteration index in the notations for conciseness. The gradient $\nabla \mathcal{L}_{\text{base}}(\theta)$ at the parameter estimate θ is:

$$\nabla \mathcal{L}_{\text{base}}(\theta) = \nabla \mathcal{L}_{\text{lsq}}(\theta) + \lambda_{\text{tran}} \nabla \mathcal{L}_{\text{tran}}(\theta). \quad (19)$$

The gradient $\nabla \mathcal{L}_{\text{lsq}}(\theta^{(d)}) = \frac{\partial}{\partial \theta} \mathcal{L}_{\text{lsq}}(\theta)$ is given by the chain rule and is calculated using the standard `grad` function in pytorch.

For the transductive loss, we first write $\mathcal{L}_{\text{tran}}(\theta) = \sum_{j=1}^{\tilde{N}} \mathcal{L}_{\text{ent}}(\tilde{s}_j(\theta))$ where \mathcal{L}_{ent} is the entropy loss as a function of the logits. It, along with its derivative, are given by,

$$\begin{aligned} \mathcal{L}_{\text{ent}}(\tilde{s}) &= \log \sum_{c=1}^k e^{\tilde{s}^c} - \frac{\sum_{c=1}^k \tilde{s}^c e^{\tilde{s}^c}}{\sum_{c=1}^k e^{\tilde{s}^c}}, \\ \frac{\partial \mathcal{L}_{\text{tran}}}{\partial \tilde{s}} &= \frac{e^{\tilde{s}}}{\sum_{c=1}^k e^{\tilde{s}^c}} \left(\frac{\sum_{c=1}^k \tilde{s}^c e^{\tilde{s}^c}}{\sum_{c=1}^k e^{\tilde{s}^c}} - \tilde{s} \right), \quad \tilde{s} \in \mathbb{R}^k. \end{aligned} \quad (20)$$

The gradient of the transductive objective can thus be expressed as,

$$\nabla \mathcal{L}_{\text{tran}}(\theta) = \sum_{j=1}^{\tilde{N}} \frac{\partial \mathcal{L}_{\text{ent}}}{\partial \tilde{s}_j} \frac{\partial \tilde{s}_j}{\partial \theta}, \quad (21)$$

where, \tilde{s}_j are the logits for the j^{th} query sample. In (21), $\partial \tilde{s}_j / \partial \theta$ is computed by a single backprop operation in pytorch. Hence, we have the full gradient $\nabla \mathcal{L}_{\text{base}}(\theta)$ at the parameter estimate θ .

Similar to the gradient, the Hessian approximation H can be written as:

$$H(\theta) = H_{\text{lsq}}(\theta) + \lambda_{\text{tran}} H_{\text{tran}}(\theta), \quad (22)$$

where H_{lsq} and H_{tran} are the Hessian approximations for the least squares loss \mathcal{L}_{lsq} and the transductive loss $\mathcal{L}_{\text{tran}}$ w.r.t. the parameter θ , respectively. The step length α is thus:

$$\alpha = \frac{\nabla \mathcal{L}_{\text{base}}(\theta)^T \nabla \mathcal{L}_{\text{base}}(\theta)}{Q_{\text{lsq}} + \lambda_{\text{tran}} Q_{\text{tran}}}. \quad (23)$$

Here $Q_{\text{lsq}} = \nabla \mathcal{L}_{\text{base}}(\theta)^T H_{\text{lsq}} \nabla \mathcal{L}_{\text{base}}(\theta)$ and, $Q_{\text{tran}} = \nabla \mathcal{L}_{\text{base}}(\theta)^T H_{\text{tran}} \nabla \mathcal{L}_{\text{base}}(\theta)$. The Hessian H_{lsq} is approximated by the Gauss-Newton approximation and provides significant computational benefits since it only involves first order derivatives. We set $H_{\text{lsq}} = J^T J$, where J is the Jacobian of the residuals in the squared objective \mathcal{L}_{lsq} at θ . Hence, $\nabla \mathcal{L}_{\text{base}}(\theta)^T H_{\text{lsq}} \nabla \mathcal{L}_{\text{base}}(\theta)$ can be computed by a double backpropagation operation in pytorch.

For the transductive loss, we first write the Hessian of $\mathcal{L}_{\text{tran}}$ as,

$$\frac{\partial^2 \mathcal{L}_{\text{tran}}(\theta)}{\partial \theta^2} = \sum_{j=1}^{\tilde{N}} \left(\frac{\partial \tilde{s}_j}{\partial \theta} \right)^T \frac{\partial^2 \mathcal{L}_{\text{ent}}}{\partial \tilde{s}^2} \Big|_{\tilde{s}_j} \left(\frac{\partial \tilde{s}_j}{\partial \theta} \right). \quad (24)$$

Here we have used (21) along with the linearity of the logits \tilde{s}_j in θ . We therefore thus only need to find a positive definite approximation of the Hessian $\frac{\partial^2 \mathcal{L}_{\text{ent}}}{\partial \tilde{s}^2}$, while the factor $\frac{\partial \tilde{s}_j}{\partial \theta}$ is computed using auto-differentiation as before. We consider a convex approximation of (20) by retaining only the first convex term while discarding the second,

$$H_{\text{ent}}(\tilde{s}) = \frac{\partial^2}{\partial \tilde{s}^2} \left(\log \sum_{c=1}^k e^{\tilde{s}^c} \right) = \text{diag}(\tilde{p}) - \tilde{p} \tilde{p}^T \text{ where,}$$

$$\tilde{p} = \text{SoftMax}(\tilde{s}) = \frac{e^{\tilde{s}}}{\sum_c \tilde{s}^c} \quad (25)$$

Here, $\text{diag}(\tilde{p})$ denotes a diagonal matrix with the elements \tilde{p} . Since, only second order information is needed to calculate the step length, we found this approximation very effective in practice. The quadratic approximation of the transductive objective can thus finally be expressed as,

$$H_{\text{tran}} = \sum_{j=1}^{\tilde{N}} \left(\frac{\partial \tilde{s}_j}{\partial \theta} \right)^T H_{\text{ent}}(\tilde{s}_j) \left(\frac{\partial \tilde{s}_j}{\partial \theta} \right). \quad (26)$$

B. Base Learner optimizer iterations during meta-training and meta-testing

Here, we provide further details regarding the analysis of the number of steepest descent optimization iterations used within the base learner (Fig. 2 and Tab. 2 in the paper). Tab. 7 presents the Fig. 2 of the main paper in tabular form together with 95% confidence intervals. It lists the 5-way, 1-shot and 5-shot test accuracy on tieredImageNet w.r.t. the number of iterations used during inference. The model employed during inference used 10 iterations during meta-training. Furthermore, Tab. 8 provides an extended version of Tab. 2 in the main paper. Tab. 8 analyzes the effect of the number of

base learner optimizer iterations during training, by reporting the test accuracy for tieredImageNet benchmark. A fixed number of 15 iterations is used during inference.

Table 7: Analysis of the number of optimization iterations used in the base learner during meta-testing.

Num. iter.	tieredImageNet 5-way	
	1-shot	5-shot
0	47.42±0.68	59.87±0.63
3	59.31±0.73	74.19±0.59
6	65.73±0.65	81.18±0.60
9	68.57±0.66	83.72±0.56
12	69.81±0.68	84.01±0.54
15	69.92±0.64	84.41±0.55
18	69.99±0.70	84.40±0.59
21	69.84±0.63	84.31±0.56
24	69.50±0.67	84.12±0.58

Table 8: Analysis of the number of optimization iterations used in the base learner during meta-training.

Num. iter.	tieredImageNet 5-way	
	1-shot	5-shot
0	65.01±0.70	81.32±0.58
1	66.47±0.72	82.01±0.57
3	67.62±0.67	82.61±0.56
5	68.73±0.66	83.14±0.54
10	69.92±0.64	84.41±0.55
15	69.56±0.68	83.82±0.54

C. Visualizing the effect of the transductive loss

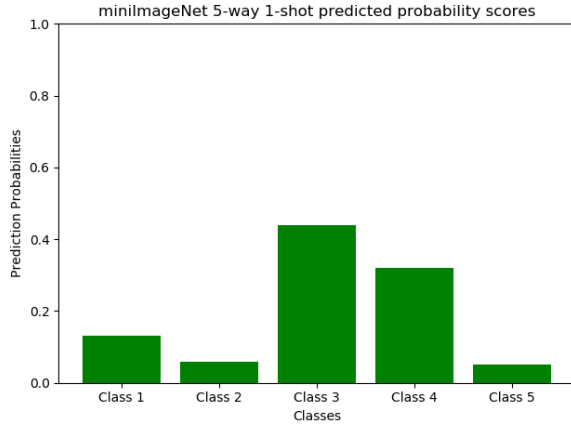
In this section, we visualize the effect of the transductive loss in 1-shot and 5-shot cases for a challenging example (Fig. 3) from the miniImageNet dataset. Fig. 4a and 4b show the softmaxed predicted scores for the mentioned 5-way 1-shot task with and without the transductive loss on the miniImageNet benchmark. When using the transductive loss, we weigh the loss by the transductive loss weight parameter λ_{tran} that is meta-learned during training. It is quite evident that transduction helps the base learner in being more confident in its predictions which is very beneficial for the 1-shot case (Sec. D). On the other hand, for the 5-shot case (Fig. 5a and 5b), we see that transduction does not have much significant effect on the softmaxed predicted scores which is reiterated in the ablations (Sec. D).

D. Additional ablations

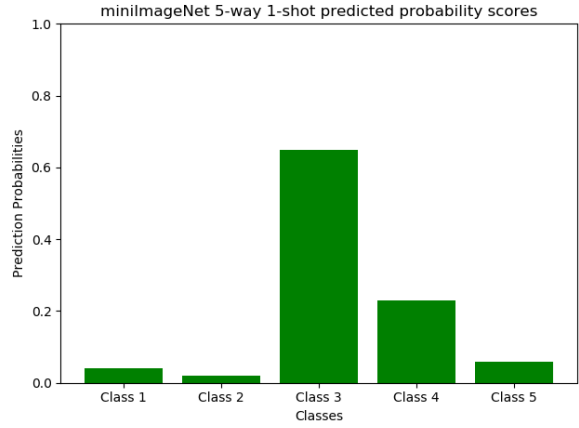
Here, we provide an ablation study for each of the major components of our approach, without the dense features. Tab. 9 shows the ablations on the tieredImageNet and the miniImageNet benchmarks. The meanings of the ablative versions of our approach remain the same as in the main text except that for **+LearnLoss** and **+Transductive**, we do not



Figure 3: Representative images of each of the classes. The left most image is representative of class 1 and the right most is representative of class 5.

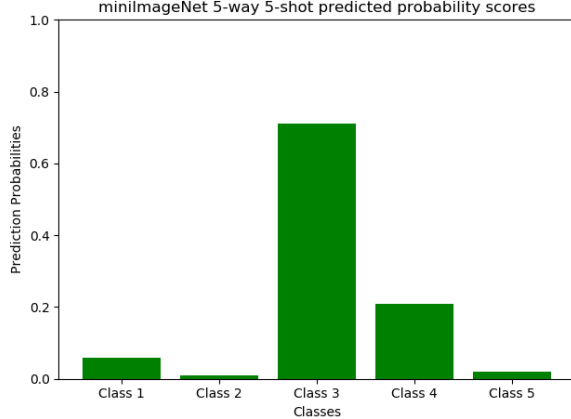


(a) Predicted probability scores without transductive loss. Class 3 is the true class

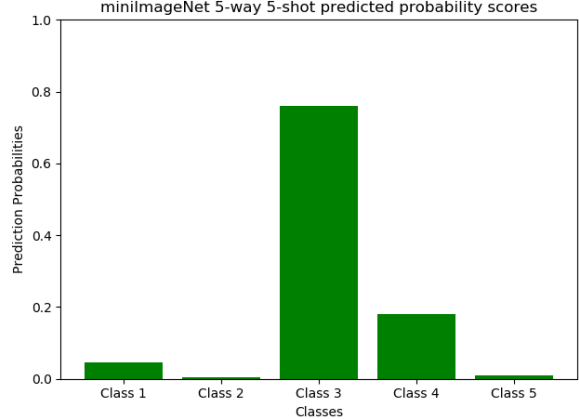


(b) Predicted probability scores with transductive loss. Class 3 is the true class

Figure 4: Effect of the transductive loss on an example 5-way 1-shot task.



(a) Predicted probability scores without transductive loss. Class 3 is the true class



(b) Predicted probability scores with transductive loss. Class 3 is the true class

Figure 5: Effect of the transductive loss on a demo 5-way 5-shot episode

include the dense features. We notice similar trends as with the dense features. **+LearnLoss** achieves a relative gain of 1% for bot, 1-shot and 5-shot test performance on tieredImageNet.

The corresponding gains are 0.9% and 0.7% for the miniImageNet benchmark. Using the transductive objective in **+Transductive** with the inductive objective, the relative

Table 9: Ablative study of our approach on tieredImageNet and miniImageNet datasets. Results are reported in terms of accuracy (%) with 95% confidence interval.

		Baseline	+Initializer	+LearnLoss	+Transductive	+Dense (FIML)
tieredImageNet	1-shot	64.73 \pm 0.73	65.32 \pm 0.71	65.97 \pm 0.72	67.91 \pm 0.69	69.92 \pm 0.64
	5-shot	80.89 \pm 0.54	81.06 \pm 0.57	81.79 \pm 0.58	82.27 \pm 0.56	84.41 \pm 0.55
miniImageNet	1-shot	61.97 \pm 0.69	62.13 \pm 0.68	62.66 \pm 0.70	63.72 \pm 0.69	65.00 \pm 0.64
	5-shot	78.12 \pm 0.48	78.56 \pm 0.45	79.12 \pm 0.46	79.47 \pm 0.47	80.52 \pm 0.43

gains over **+LearnLoss** for 1-shot and 5-shot test performance on tieredImageNet are 2.9% and 0.6%, respectively. For miniImageNet, the corresponding relative gains are 1.7% and 0.4%, respectively. The transductive objective is given more weightage by the meta-learner for a 1-shot case than for a 5-shot case as explained in the main paper. Finally, we list the test accuracy for our final version **+Dense (FIML)** that imbibes dense features in the pipeline.